CCS Chemistry

RESEARCH ARTICLE

Received: Sept. 14, 2018 | Accepted: Nov. 13, 2018 | Published: June 4, 2019

In Situ Loading and Delivery of Short Single- and Double-Stranded DNA by Supramolecular Organic Frameworks

Bo Yang[1], Xiao-Dan Zhang[2], Jian Li[3], Jia Tian[1], Yi-Peng Wu[1], Fa-Xing Yu[3], Ruibing Wang[4]*, Hui Wang[1], Dan-Wei Zhang[1], Yi Liu[5]*, Lu Zhou[2]* & Zhan-Ting Li[1]*

[1]*Department of Chemistry, Shanghai Key Laboratory of Molecular Catalysis and Innovative Materials and Collaborative Innovation Center of Chemistry for Energy Materials (iChEM), Fudan University, Shanghai 200438 (China),* [2]*Department of Medicinal Chemistry, School of Pharmacy, Fudan University, Shanghai 201203 (China),* [3]*Children's Hospital and Institutes of Biomedical Sciences, Fudan University, Shanghai 200032 (China),* [4]*State Key Laboratory of Quality Research in Chinese Medicine, Institute of Chinese Medical Sciences, University of Macau, Taipa, Macao (China),* [5]*The Molecular Foundry, Lawrence Berkeley National Laboratory, Berkeley, CA 94720 (USA)*

**Corresponding authors: ztli@fudan.edu.cn; zhoulu@fudan.edu.cn; rwang@umac.mo; yliu@lbl.gov*

Cite this: *CCS Chem.* **2019**, *1*, 156–165

Short DNA represents an important class of biomacromolecules that are widely applied in gene therapy, editing, and modulation. However, the development of simple and reliable methods for their intracellular delivery remains a challenge. Herein, we describe that seven water-soluble, homogeneous supramolecular organic frameworks (SOFs) with a well-defined pore size and high stability in water that can accomplish in situ inclusion of single-stranded (ss) and double-stranded (ds) DNA (21, 23, and 58 nt) and effective intracellular delivery (including two noncancerous and six cancerous cell lines). Fluorescence quenching experiments for single and double end-labeled ss- and ds-DNA support that the DNA sequences can be completely enveloped by the SOFs. Confocal laser scanning microscopy and flow cytometry reveal that five of the SOFs exhibit excellent delivery efficiencies that, in most of the studied cases, outperform the commercial standard Lipo2000, even at low SOF–nucleic acid ratios. In addition to high delivery efficiencies, the water-soluble, self-assembled SOF carriers have a variety of advantages, including convenient preparation, high stability, and in situ DNA inclusion, which are all critical for practical applications in nucleic acid delivery.

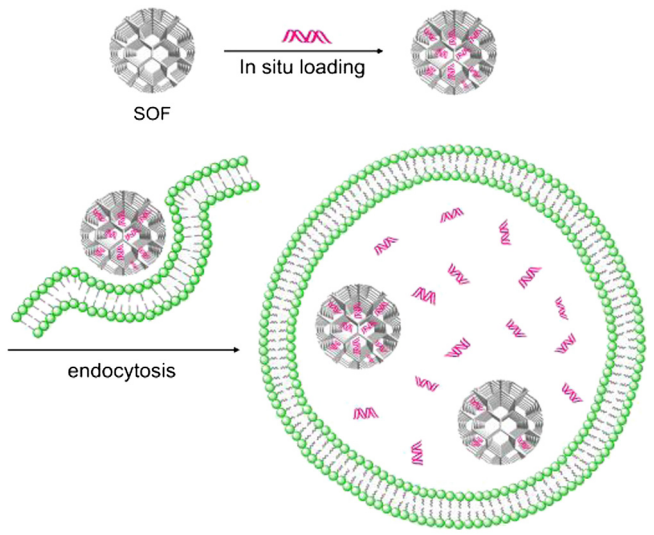

Keywords: nucleic acid delivery, homogeneous carrier, electrostatic interaction, self-assembly, porous polymer

DOI: 10.31635/ccschem.019.20180011
CCS Chem. **2019**, *1*, 156–165

Introduction

Intracellular delivery of exogenous DNA is of paramount importance for the development of gene therapy and editing.[1–4] Owing to their potential clinical applications, short DNA strands have been important targets of delivery studies.[5–8] Viral vectors have been demonstrated to be highly efficient, but suffer from safety concerns, high cost, and scale-up difficulty.[9–11] In the past two decades, nonviral, cationic vectors (that may interact with DNA through multivalent electrostatic interactions), including liposomes,[12–14] dendrimers,[15–18] polymers,[19–24] and nanoparticles,[25–28] have been extensively investigated and have achieved considerable success in gene delivery. However, relatively high cytotoxicity, limited delivery efficiency, and lack of precision remain as obstacles to their reaching the clinical trial stage. Materials with defined porosity are structurally suitable for DNA inclusion because their inherent pores are expected to avoid unnecessary entanglement of incorporated DNA strands, which may restrain gene release. Nevertheless, previously reported vectors of this class of materials have been limited to solid-state structures,[29–31] the slow metabolism of which may cause detrimental internal aggregation. The development of water-soluble, cationic porous frameworks that are able to behave in a homogeneous manner is expected to combine the advantages of both viral and nonviral vectors.

Recently, we developed a general strategy for the generation of water-soluble, three-dimensional supramolecular organic frameworks (SOFs) from the co-assembly of pre-organized multi-cationic monomers with cucurbit[8]uril (CB[8]).[32–37] As a family of self-assembled, water-soluble, porous polyelectrolytes, diamondoid SOFs were demonstrated to adsorb anionic guests and deliver adsorbed chemotherapeutic reagents, such as pemetrexed, into tumor cells.[38] Herein, we describe seven SOFs, with a pore size of approximately 2.0–2.2 nm, that can incorporate short single - or double-stranded (ss- or ds-) DNA (21, 23, and 58 nt) in a facile manner by simply mixing the two species together and deliver the DNA strands into noncancerous and cancerous cells. We demonstrate that of the 126 delivery experiments, 98 cases achieved a delivery efficacy surpassing that of Lipo2000, a gold-standard commercial delivery reagent.

Results and Discussion

Diamondoid SOFs are regular porous supramolecular polyelectrolytes co-assembled by tetracationic monomers and CB[8].[32] With (4-phenyl)pyridinium as the binding subunit through the CB[8] encapsulation-enhanced dimerization binding motif, which has found wide applications in supramolecular self-assembly,[39–50] the

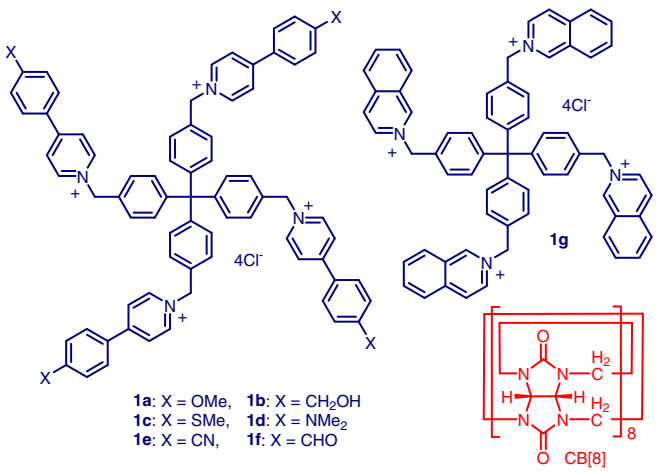

Figure 1 | *The structures of compounds **1a–g** and CB[8].*

water-soluble, polycationic frameworks form ordered pores that have a size of approximately 2.2 nm.[32] Previously, we demonstrated their robustness as molecular drug carriers to attain intracellular transport and low cytotoxicity.[38,51] Given the polyanionic feature of DNA and the approximately 2.0 nm diameter of dsDNA,[52,53] we hypothesized that diamondoid SOFs would be suitable carriers for the inclusion of both short ssDNA, with smaller diameter as compared to dsDNA, and dsDNA through multivalent electrostatic interactions,[54,55] which is the basis for all reported polycationic DNA carriers. The homogeneity of SOFs was expected to allow for quick DNA inclusion and reversible release after intracellular delivery. **SOF-a–g**, constructed from **1a–g** and CB[8] (1:2), were thus used to exploit this potential (Figure 1). The first six frameworks have been reported for the inclusion of discrete organic guests and for SOF post-modification,[32,56] while **SOF-g** was designed to test the generality of this new delivery strategy.

The synthesis and characterization of the new **SOF-g** is discussed here in detail, whereas **SOF-a-f** preparation and characterization have been reported previously.[32,38] Tetrahedral monomer **1g** was prepared from tetrakis(4-(bromomethyl)phenyl)-methane and isoquinoline, followed by separation ion-exchange chromatography. **SOF-g** was prepared by dissolving a 1:2 (molar ratio) mixture of **1g** and CB[8] in hot water. The X-ray crystallographic structure of the 2:1 mixture of *N*-benzylisoquinolinium bromide (**2**) with CB[8] revealed that two isoquinolinium moieties were entrapped in the cavity of the CB[8] (Supporting Information Figure S1), which evidenced the 2:1 binding motif of **1g** and CB[8]. ^{1}H NMR titration experiments in D_2O for **2** and **1g** with CB[8] further supported this 2:1 binding motif in water (Supporting Information Figure S2). Isothermal titration calorimetry gave (apparent) binding constants of 4.8×10^{11} M^{-2} for $[\mathbf{2}]_2$cCB[8] and 2.5×10^{12} M^{-2} for the 2:1 complex of the appended isoquinolinium subunits of

DOI: 10.31635/ccschem.019.20180011
CCS Chem. **2019**, *1*, 156–165

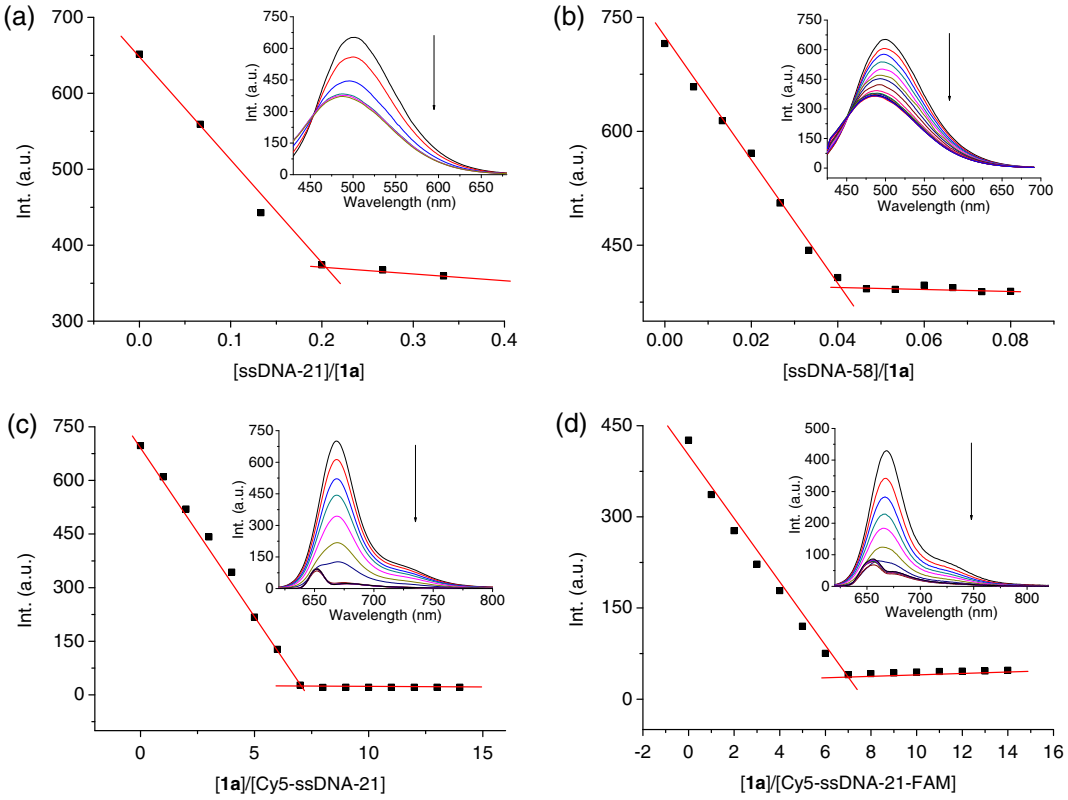

Figure 2 | *Fluorescence quenching plots of **SOF-a** ([**1a**] = 5.0 μM, λ = 500 nm) in water with the addition of (a) ssDNA-21 and (b) ssDNA-58. **SOF-a**-induced fluorescence quenching plots of (c) Cy5-ssDNA-21 (λ = 670 nm) and (d) Cy5-ssDNA-21-FAM (Cy5, λ = 670 nm), highlighting a clear inflection point in every titration.*

1g and CB[8], respectively (Supporting Information Figure S3), suggesting high stability of this binding motif and positive cooperativity for the appended isoquinolinium subunits of **1g**.[32] Two-dimensional, ^{1}H NMR diffusion-ordered spectroscopic experiments for the mixture of **2** (2:1) and **1g** (0.5:1) with CB[8] (1.0 mM) in D_2O gave rise to a diffusion coefficient (D) of 2.5×10^{-10} and 1.1×10^{-10} $m^2\,s^{-1}$ for the signals of both components (Supporting Information Figure S4), indicating that **1g** and CB[8] formed larger supramolecular entities. Dynamic light-scattering experiments for the 1:2 solutions of **1g** and CB[8] revealed the formation of large aggregates, with the hydrodynamic diameter (D_H) ranging from 31 nm (CB[8] = 0.03 mM) to 91 nm (CB[8] = 2 mM) (Supporting Information Figure S5). Moreover, the D_H values underwent few changes after the solutions were left to stand for 48 h, implying their high stability. Solution-phase, synchrotron small-angle X-ray-scattering (SAXS) profile of the 1:2 solution of **1g** and CB[8] (2.0 mM) exhibited a very weak and broad, but reproducible, peak corresponding to the d-spacing around 3.4 nm (Supporting Information Figure S6a). This spacing matched with the calculated {110} spacing (3.4 nm) of the modeled **SOF-g** network (Supporting Information Figure S7), reflecting its periodicity in water. The solid-phase, synchrotron SAXS profile afforded quite a sharp signal at 2.0 nm, which matched well with the calculated {211} spacing (Supporting Information Figure S6b). Moreover, the solid-phase, synchrotron small-angle X-ray diffraction profile exhibited three broad peaks around 2.8, 1.4, and 0.83 nm (Supporting Information Figure S6c), which matched with the calculated {111}, {222}, and {334} spacings. The structural features of SOF-g are similar to those of other SOFs assembled in a similar manner.[32,36] With the framework structure confirmed, it's in vitro cytotoxicity was evaluated using human cancer (HeLa) cells via a Cell Counting Kit-8 assay (Supporting Information Figure S8). It was found that, after incubation for 24 h with **SOF-g** at 35, 180, 370, and 740 μg/mL, the viability of the HeLa cells were maintained at 89.1–97.0%, 96.1–100%, 97.0–100%, and 98.0–100%, respectively, showing the low cytotoxicity of this new self-assembled framework, which is similar to those of the **SOFs-a–f** reported previously.[38]

All the tetrahedral monomers and the corresponding **SOF-a–g** exhibited strong fluorescence. To investigate the inclusion of the DNA in the SOFs, the SOF fluorescence was then recorded with incremental addition of six strands of ss- and ds-DNA (ssDNA-21, ssDNA-23, ssDNA-58, dsDNA-21, dsDNA-23, and dsDNA-58, the numeric

DOI: 10.31635/ccschem.019.20180011
CCS Chem. **2019**, *1*, 156–165

suffix representing the number of nucleotides in the sequence; Figure 2a,b; Supporting Information Table S1 and Figure S9a–d). For all of these experiments, the concentrations of the SOFs were kept constant ([**1a–g**] = 5.0 or 2.5 μM). Adding the DNA samples to the solution of the SOFs induced significant quenching (**SOF-a**,**b**,**g**) or enhancement (**SOF-c–f**) of the emission of the SOF (Supporting Information Figures S10 and S11). Moreover, at both concentrations of the frameworks, this emission quenching or enhancement exhibited a discernible inflection, which corresponded to saturated DNA loading. In contrast, adding excess of monosodium phosphate induced no significant change of the emission of the frameworks (Supporting Information Figure S12). These observations supported that both ss- and ds-DNA were included into the interior of the SOFs through multivalent electrostatic interaction, even though hydrophobic interaction could not be excluded (Figure 3).[54,55] Assuming the concentration of the DNA at the inflection point to be the saturation inclusion concentration, the weight percent (wt%) of the DNA included by the SOFs can be calculated (Supporting Information Tables S2 and S3). It was found that at [**1**] = 5.0 μM, the SOF carriers could include 18–70 wt% of ssDNAs and 14–32 wt% of dsDNAs, whereas at [**1**] = 2.5 μM, the values were 12–43 and 19–32 wt%, respectively.

The fluorescence quenching of single and double end-labeled DNA strands (Cy5-ssDNA-21, Cy5-ssDNA-58, Cy5-ssDNA-21-FAM, HEX-ssDNA-21-Cy5, Cy5-ssDNA-58-FAM, Cy5-dsDNA-21-FAM, and Cy5-dsDNA-58-FAM) (Supporting Information Table S1) by the SOFs was also investigated. In all of the cases, the quenching of the fluorescence probes all displayed an inflection when about 6–68 molar equivalents of tetrahedral **1a–g** of SOFs were added (Figure 2c,d; Supporting Information Figures S9 and S13–S24), and the longer DNA required more equivalents of SOFs for reaching the saturation. When normalized by the cation/anion charge ratio, the above equivalence translates to a ratio of 1.0:2.3 between the total cation concentration of the SOFs and the total anion concentration of the DNA strands. In contrast, under the identical conditions, adding SOFs to the solution of the simple molecular dyes Cy5, FAM, or HEX of the same concentration caused very little quenching of their emission. Thus, the above results strongly support that both single ss- and ds-DNA were effectively included in the interior of the frameworks to reach a charge balance (Figure 3).

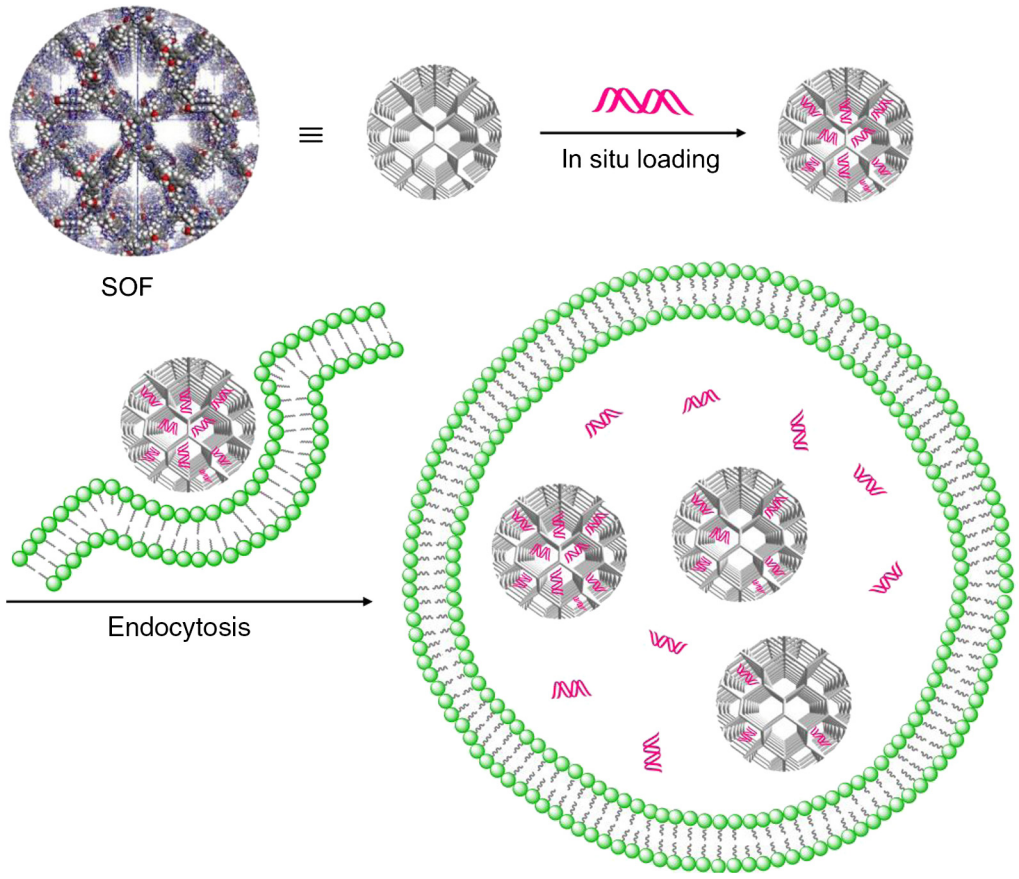

Figure 3 | *Schematic representation of the in situ loading and delivery of DNA by polycationic SOFs.*

DOI: 10.31635/ccschem.019.20180011
CCS Chem. **2019**, *1*, 156–165

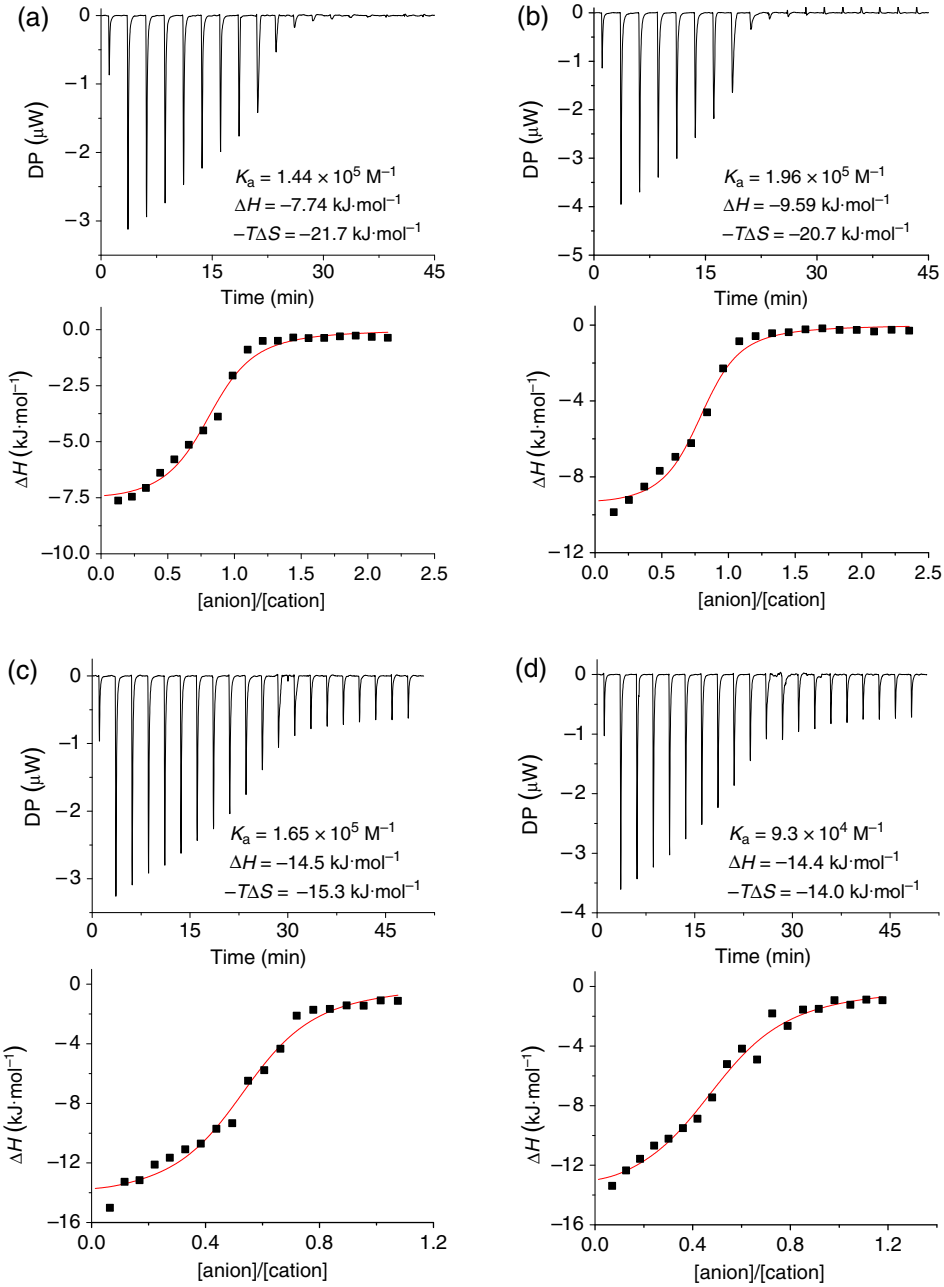

Figure 4 | *Isothermal titration thermograms of (a) ssDNA-21 ([anion] = 2.1 mM), (b) ssDNA-23 ([anion] = 2.3 mM), (c) dsDNA-21 ([anion] = 0.84 mM), and (d) dsDNA-23 ([anion] = 0.92 mM) into the solution of* ***SOF-a*** *([cation] = 0.20 mM) at 25 °C. The injection volume of the DNAs was 2 μL. [anion] represents the total phosphate concentration of the DNA, and [cation] represents the total pyridinium concentration of* ***SOF-a****.*

To quantitatively evaluate the inclusion of the DNA into SOFs,[57] isothermal calorimetric (ITC) experiments were performed for **SOF-a** and **SOF-g** and the above six ss- and ds-DNA strands (Figure 4; Supporting Information Figure S25a–d). As the inclusion occurred homogeneously, it was expected that, once included into the interior of the frameworks, linear nucleic acids might adopt extended or crooked conformations. Control ITC experiments revealed that neither monosodium phosphate nor simple nucleotides interacted with SOFs. Thus, the strong interactions between SOFs and nucleic acids are likely attributed to mainly the multivalent electrostatic interactions between the pyridinium or isoquinolinium cations and the phosphate anions of nucleic acids. As a simplified treatment of the complicated binding event, the total cation and anion concentrations of the two respective species were kept at a 1:1 ratio. The titration data were subsequently used to derive apparent binding constants for the ion-pair complexes of ssDNA-21⊂**SOF-a**, ssDNA-23⊂**SOF-a**, dsDNA-21⊂**SOF-a,** and dsDNA-21⊂**SOF-a**

DOI: 10.31635/ccschem.019.20180011
CCS Chem. **2019**, *1*, 156–165

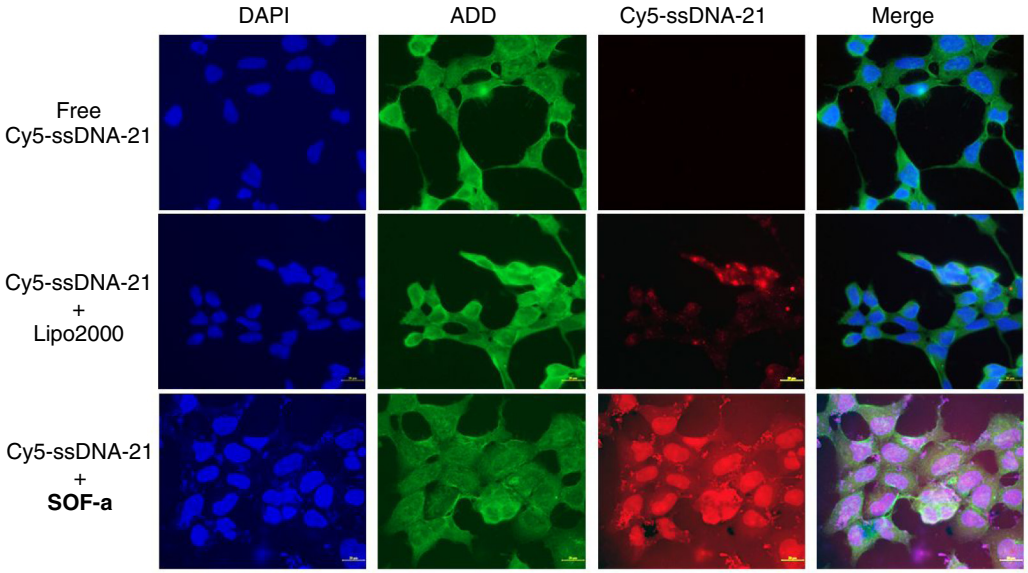

Figure 5 | *Confocal laser scanning microscopic images of 293A cells after incubation for 2 h with Cy5-ssDNA-21, Cy5-ssDNA-21⊂Lipo2000, and Cy5-ssDNA-21⊂**SOF-a**. The amounts of ssDNA, Lipo2000, and **SOF-a** used were 2.5, 7.0, and 7.0 μg, respectively. Nuclei were stained with DAPI (blue), and cells were stained with ADD (green).*

to be 1.44×10^5, 1.96×10^5, 1.65×10^5, and 9.3×10^4 M^{-1}, respectively. For the four ion-pair complexes of **SOF-g**, the binding constants were determined to be 5.35×10^5, 2.66×10^5, 2.39×10^6, and 5.85×10^6 M^{-1}, respectively. All the results indicated strong binding of SOFs toward the DNA. Titration experiments were also conducted for longer ssDNA-58, which exhibited more complicated exo- and endothermic phenomena and could not be treated as for the shorter ones (Supporting Information Figure S25e). The ITC experiments also revealed that, for all the systems studied, the inclusion was driven enthalpically and entropically. The enthalpic contribution should come from the enhanced intermolecular ion-pair interaction, whereas the entropic contribution could be rationalized by considering that the included DNA might, to a great extent, cover the hydrophobic surfaces of the SOFs and consequently release the high-energy water molecules of low freedom from the hydrophobic surfaces.[58]

Previous studies demonstrated that SOFs could quickly enter cells after incubation and deliver dianionic pemetrexed into tumor cells through endocytosis.[35] The intracellular delivery of SOFs loaded with short DNA strands was then investigated using Cy5-labeled ssDNA (Cy5-ssDNA-21) with the 293A cell line by staining the nuclei with 4′,6-diamidino-2-phenylindole (DAPI) and the cells with adducin α-antibody (H-100, ADD), respectively. After incubation with Cy5-ssDNA-21⊂**SOF-a** (0.25 and 14.0 μg, respectively) for 2 h, the cells were examined by confocal laser scanning microscopy. It was found that the fluorescence signal of the Cy5 dye was very clear and highly overlapped with that of DAPI-stained nuclei and ADD-stained cells. In contrast, in the absence of **SOF-a**, no fluorescence of the Cy5 dye was observed for free Cy5-ssDNA-21 of the identical dosage (Supporting Information Figure S26), clearly supporting that **SOF-a** was capable of delivering Cy5-ssDNA-21 into 293A cells. We further examined the delivery of higher load of Cy5-ssDNA-21 (2.5 μg) into 293A cells by **SOF-a** and the commercial reagent Lipo2000, respectively, at the equivalent dosage (7.0 μg) in the presence of fetal bovine serum (5%). As expected, within the time studied (up to 2 h), no endocytosis of Cy5-ssDNA-21 (2.5 μg) was observed in the absence of added carriers. For cells treated with Lipo2000 loaded with Cy5-ssDNA-21, weak fluorescence of the Cy5 dye was observed in the cells within 1 h of incubation; however, no uniform delivery could be achieved even after incubation for 2 h (Figure 5; Supporting Information Figure S27). In contrast, with the treatment of **SOF-a** loaded with Cy5-ssDNA-21 at the same dosage, the fluorescence of the Cy5 dye was considerably stronger and uniform delivery was observed after incubation within 2 h.

The intracellular delivery of DNA using SOF carriers was further determined using flow cytometry. Measurement was first conducted with Cy5-ssDNA-21 (2.5 μg) for the 293A cell line. Again, Lipo2000 (7.0 μg) was used for comparison, and the flow cytometry measurements were conducted after incubation in 10% fetal bovine serum for 15 min, 1 h, and 2 h to gain insight into the delivery process (Figure 6a; Supporting Information Figure S28). In the absence of a carrier, no intracellular DNA delivery was observed, as evidenced by the absence of the fluorescence of Cy5. After incubation for 15 min, Lipo2000 and

DOI: 10.31635/ccschem.019.20180011
CCS Chem. **2019**, *1*, 156–165

SOF-a,b,d–g (7.0 μg) induced 0.1–8.9% delivery or internalization efficiency, which was defined as the percentage of cells that internalized the DNA among all the cells tested, respectively, suggesting their low delivery efficacy, whereas **SOF-c** realized a remarkable 45.2% delivery efficiency. After incubation for 1 and 2 h, the delivery efficiencies of **SOF-c** reached 93% and 98.9%, respectively, which were again significantly higher than that of Lipo2000 (27.2% and 57.5%, respectively). These data have also shown very good repeatability (Supporting Information Figure S29). Control experiments show that under identical experimental conditions, tetrahedral monomers **1a–g** exhibited limited delivery efficiencies (Supporting Information Figure S30) with **1a** and **1c** showing the highest efficiencies of 19.1–27.7% and 13.2–17.7%, respectively. This result strongly supports that the porous architectures of **SOF-a–g** remarkably enhanced their capacity of including, delivering, and transfecting nucleic acids.

Because **SOF-b** and **SOF-d** generally exhibited the lowest delivery efficiency, we subsequently focused on **SOF-a,c,e–g** and extended the investigation to determine their potential for transfecting Cy5-ssDNA-21 (2.5 μg) into different cell lines, including human pancreatic ductal epithelial (HPDE) and six cancer cell lines (PANC-1, Capan-1, SiHA, H1299, HeLa, and CaCo-2). The measurements were performed after incubation in 10% phosphate-buffered saline (PBS) for 2 h (Figure 6d; Supporting Information Figures S31–S34). In the blank test without the carriers, about 5% of HeLa cells were transfected by passive transportation of the nucleic acid, whereas all other cell lines underwent less than 1% of delivery. With Lipo2000 (7.0 μg) as the carrier, the delivery efficiency of the seven cell lines was 80.0–81.9%, 20.3–33.0%, 64.5–68.3%, 73.6–76.6%, 70.0–81.9%, 66.4–69.1%, and 13.3–16.1%, respectively. With SOFs (7.0 μg) as the carriers, in all 35 SOF studies (combinations of SOF and cell lines), 32 systems displayed delivery efficiency that was higher than that of Lipo2000 for the same cell line, except for that of H1299 by **SOF-e** (61.9–68.5%) and **SOF-f** (68–76.3%) and CaCo-2 by **SOF-a** (8.4–9.6%). Moreover, for all the seven cell lines, the delivery

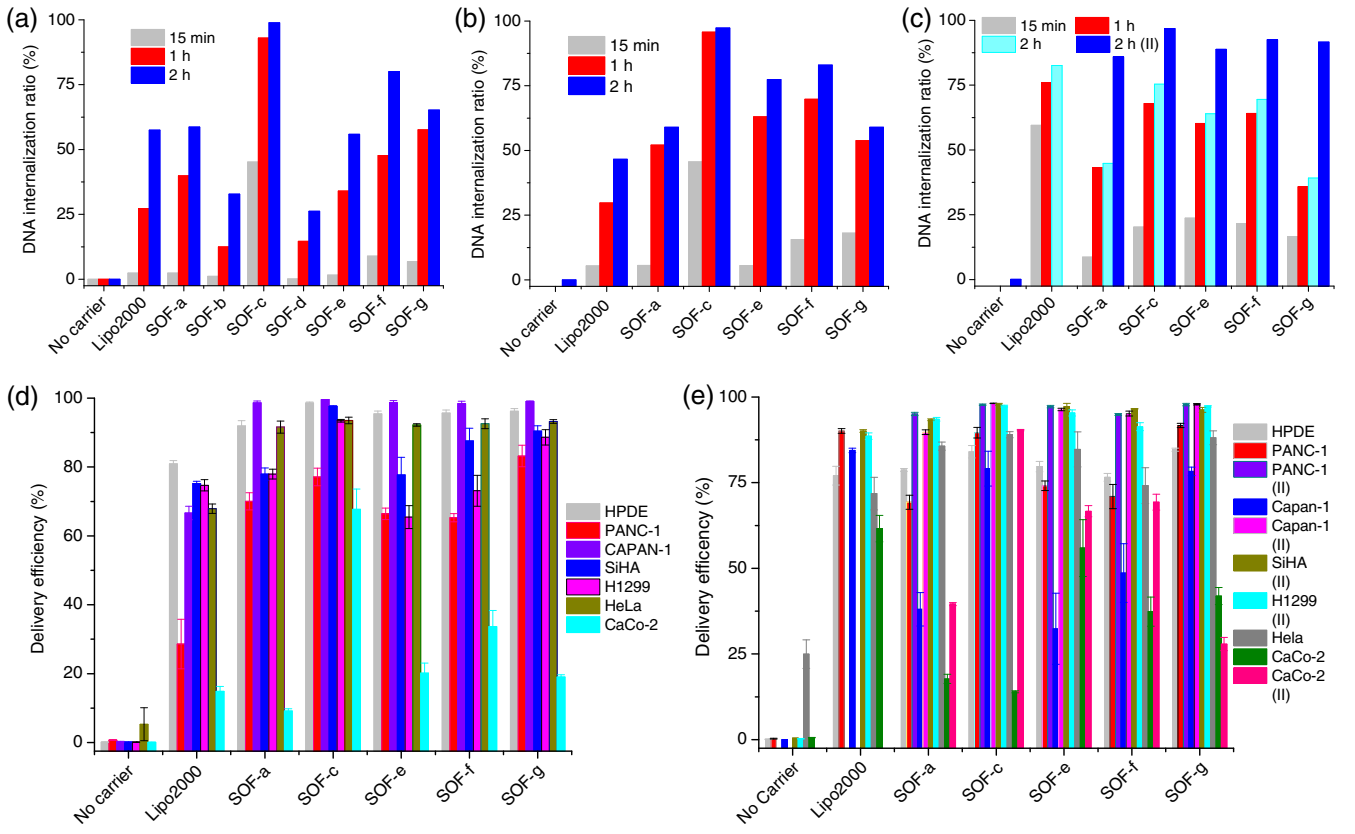

Figure 6 | *Delivery (internalization) experiment of Cy5-labeled DNA by SOFs: (a) Cy5-ssDNA-21 (2.5 μg) by **SOF-a–g** (7.0 μg) in 293A cell line, (b) Cy5-dsDNA-21 (4.8 μg) by **SOF-a,c,e–g** (7.0 μg) in 293A cell line, (c) Cy5-dsDNA-58 (4.8 μg) by **SOF-a,c,e–g** (7.0 or 56 μg for blue) in 293A cell line, (d) Cy5-ssDNA-21 (2.5 μg) by **SOF-a,c,e–g** (7.0 μg) in HPDE, PANC-1, Capan-1, SiHA, H1299, HeLa, and CaCo-2 cell lines after incubation in 10% PBS for 2 h, and (e) Cy5-dsDNA-21 (4.8 μg) by **SOF-a,c,e–g** (7.0 or 14.0 μg) for HPDE, PANC-1, Capan-1, SiHA, H1299, HeLa, and CaCo-2 cell lines after incubation in 10% PBS for 2 h. Lipo2000: 7.0 μg for ssDNA and 14.0 μg for dsDNA. II: 14.0 μg of SOFs. The error bars represent that of three experiments.*

DOI: 10.31635/ccschem.019.20180011
CCS Chem. **2019**, *1*, 156–165

efficiencies of **SOF-c** and **SOF-g** were always higher than that of Lipo2000. In addition, among the 35 series, 19 studies reached >90% of delivery efficiency and 10 studies reached >95% of delivery efficiency.

The intracellular delivery of the above five SOF carriers for Cy5-dsDNA-21 (4.8 μg), which is composed of Cy5-ssDNA-21 and the complementary ssDNA of 21 nt, into 293A cell line was subsequently investigated (Figure 6b; Supporting Information Figure S35). A blank test showed that the delivery of the cells by passive diffusion of the nucleic acid was negligible. A preliminary test showed that the delivery efficiency of Lipo2000 (7.0 μg) was considerably lower, and thus, its amount was increased to 14.0 μg, whereas the mass of the SOF carriers remained unchanged (7.0 μg). However, in all cases detected at different time points (15 min, 1 h, and 2 h of incubation), the five SOF carriers still exhibited higher delivery efficiencies than Lipo2000. Remarkably, **SOF-c** realized 95.7% and 97.3% delivery efficiencies after incubation for 1 and 2 h, respectively. The other four SOFs induced 59–83% delivery efficiencies after incubation for 2 h, whereas in the same timeframe, Lipo2000 only reached a delivery efficiency of 46.6%.

The delivery of the five SOFs for HPDE, PANC-1, Capan-1, SiHA, H1299, HeLa, and CaCo-2 cell lines was further tested, respectively (Figure 6e; Supporting Information Figures S36–S39). For this series of experiments, the amounts of Cy5-dsDNA-21 and Lipo2000 were also maintained at 4.8 and 14.0 μg, whereas the SOF carriers were tested at two doses, 7.0 and 14.0 μg. Lipo2000 exhibited a 60.6–90.1% delivery efficiency. Compared with that of Lipo2000 for the same cell line, 34 out of the total 50 SOF samples exhibited higher delivery efficacy, with 14 reaching over 90% delivery efficacy. Among the 25 samples using 14.0 μg of SOFs, 23 exhibited a higher delivery efficiency than that of the Lipo2000 reference.

Finally, we also tested the delivery of the longer Cy5-dsDNA-58 in the 293A cell line, which is composed Cy5-ssDNA-58 and the corresponding unlabeled complementary nucleic acid of 58 nt (Figure 6c; Supporting Information Figures S40–S42). At the respective dose of 4.8, 14.0, and 7.0 μg for DNA, Lipo2000 and SOFs, the delivery efficiencies of the five SOFs were all lower than that of Lipo2000 after 15 min, 1 h, or 2 h of incubation. However, when the dose of SOFs was increased to 56.0 μg, their delivery efficiencies, after incubation for 2 h, all surpassed that of Lipo2000 (82.6%), with **SOF-c** realizing the highest efficiency of 96.8%.

The driving forces for the inclusion of DNA strands by SOFs were mainly electrostatic attraction and hydrophobicity. Both ss- and ds-DNA of 21 and 58 nt have been confirmed to be included completely by the new self-assembled carriers, suggesting that other short DNA strands with nucleotide numbers between these two can also be included to the interior of the carriers. Because the inclusion occurs homogeneously, the release of the included DNA strands should highly depend on the above two interactions. The dynamic feature of this inclusion process suggests that the included DNA could be released through simple diffusion. Previous in vitro fluorescence imaging of **SOF-a** showed that the framework accumulated in tumor cells and was subsequently metabolized or degraded in cells.[38] Thus, another important route for the release of the included DNA was through the decomposition of the framework. The above confocal laser scanning microscopy experiments also indicated that the labeled DNAs diffused into all the area of the nuclei, as observed for the delivery of small molecular drugs.

Conclusion

In summary, we have demonstrated that water-soluble SOFs can efficiently incorporate short DNA strands in a homogeneous and in situ loading manner and realize intracellular delivery into both noncancerous and cancerous cells. With the identical carrier loading, in most of the tested cases, SOFs exhibit higher delivery efficiency than the commercial reagent Lipo2000 that has often been used as the "gold standard" of nonviral gene vector, with **SOF-c** exhibiting the most promising delivery efficiency. These water-soluble, self-assembled entities represent a novel class of off-the-shelf gene delivery carriers that feature simple components, facile formulation, high stability at ambient temperature, and in situ loading of DNA. In the future, this promising strategy will be further explored for the delivery of small interfering RNA.

Conflict of Interest

The authors declare no competing financial interests.

Supporting Information

Supporting information is available.

Acknowledgments

We thank the National Natural Science Foundation of China (Nos. 21432004 and 21529201) for financial support, Shanghai Synchrotron Radiation Facility for providing BL16B1 and BL14B1 beamlines for collecting the synchrotron X-ray-scattering and diffraction data, and the SIBYLS Beamline 12.3.1 of the Advanced Light Source (ALS), Lawrence Berkeley National Laboratory, for collecting solution-phase, synchrotron small-angle X-ray-scattering data. Y. L. thanks the support from the Molecular Foundry, Lawrence Berkeley National Laboratory, supported by the Office of Science, Office of Basic Energy Sciences, Scientific User Facilities Division, of the

DOI: 10.31635/ccschem.019.20180011
CCS Chem. **2019**, *1*, 156–165

U.S. Department of Energy under Contract No. DE-AC02-05CH11231. The SIBYLS Beamline at ALS was supported through the Integrated Diffraction Analysis Technologies (IDAT) program, supported by DOE Office of Biological and Environmental Research. Additional support comes from the National Institute of Health project MINOS (R01GM105404).

References

1. Kay, M. A. State-of-the-Art Gene-Based Therapies: The Road Ahead. *Nat. Rev. Genet.* **2011**, 12, 316–328.
2. Clarke, D. T. W.; McMillan, N. A. J. Cell-Specific Therapy on Target. *Nat. Nanotechnol.* **2014**, 9, 568.
3. Wang, H.-X.; Li, M.; Lee, C. M.; Chakraborty, S.; Kim, H.-W.; Bao, G.; Leong, K. W. Crispr/Cas9-Based Genome Editing for Disease Modeling and Therapy: Challenges and Opportunities for Nonviral Delivery. *Chem. Rev.* **2017**, *117*, 9874–9906.
4. Kuşcu, L.; Sezer, A. D. Future Prospects for Gene Delivery Systems. *Exp. Opin. Drug Deliv.* **2017**, *14*, 1205–1215.
5. Southwell, A. L.; Skotte, N. H.; Bennett, C. F.; Hayden, M. R. Antisense Oligonucleotide Therapeutics for Inherited Neurodegenerative Diseases. *Trends Mol. Med.* **2012**, *18*, 634–643.
6. Fichou, Y.; Férec, C. The Potential of Oligonucleotides for Therapeutic Applications. *Trends Biotechnol.* **2006**, *24*, 563–570.
7. Ren, K.; Liu, Y.; Wu, J.; Zhang, Y.; Zhu, J.; Yang, M.; Ju, H. A DNA Dual Lock-and-Key Strategy for Cell-Subtype-Specific siRNA Delivery. *Nat. Commun.* **2016**, *7*, 13580.
8. Shipman, S. L.; Nivala, J.; Macklis, J. D.; Church, G. M. CRISPR–Cas Encoding of a Digital Movie into the Genomes of a Population of Living Bacteria. *Nature* **2017**, *547*, 345.
9. Robbins, P. D.; Ghivizzani, S. C. Viral Vectors for Gene Therapy. *Pharmacol. Therapeut.* **1998**, *80*, 35–47.
10. Finer, M.; Glorioso, J. A Brief Account of Viral Vectors and Their Promise for Gene Therapy. *Gene Ther.* **2017**, *24*, 1.
11. DiCarlo, J. E.; Deeconda, A.; Tsang, S. H. Viral Vectors, Engineered Cells and the CRISPR Revolution. In *Precision Medicine, CRISPR, and Genome Engineering*; Springer: Cham, Switzerland, **2017**; pp 3–27.
12. Torchilin, V. P. Multifunctional, Stimuli-Sensitive Nanoparticulate Systems for Drug Delivery. *Nat. Rev. Drug Discov.* **2014**, *13*, 813.
13. Buyens, K.; De Smedt, S. C.; Braeckmans, K.; Demeester, J.; Peeters, L.; van Grunsven, L. A.; du Jeu, X. D. M.; Sawant, R.; Torchilin, V.; Farkasova, K. Liposome Based Systems for Systemic siRNA Delivery: Stability in Blood Sets the Requirements for Optimal Carrier Design. *J. Controlled Release* **2012**, *158*, 362–370.
14. Chen, Z.; Liu, F.; Chen, Y.; Liu, J.; Wang, X.; Chen, A. T.; Deng, G.; Zhang, H.; Liu, J.; Hong, Z. Targeted Delivery of CRISPR/Cas9-Mediated Cancer Gene Therapy Via Liposome-Templated Hydrogel Nanoparticles. *Adv. Funct. Mater.* **2017**, *27*, 1703036.
15. Yang, J.; Zhang, Q.; Chang, H.; Cheng, Y. Surface-Engineered Dendrimers in Gene Delivery. *Chem. Rev.* **2015**, *115*, 5274–5300.
16. Paleos, C. M.; Tsiourvas, D.; Sideratou, Z. Molecular Engineering of Dendritic Polymers and Their Application as Drug and Gene Delivery Systems. *Mol. Pharmaceutics* **2007**, *4*, 169–188.
17. Wang, M.; Liu, H.; Li, L.; Cheng, Y. A Fluorinated Dendrimer Achieves Excellent Gene Transfection Efficacy at Extremely Low Nitrogen to Phosphorus Ratios. *Nat. Commun.* **2014**, *5*, 3053.
18. Zhou, Y.; Huang, W.; Liu, J.; Zhu, X.; Yan, D. Self-Assembly of Hyperbranched Polymers and Its Biomedical Applications. *Adv. Mater.* **2010**, *22*, 4567–4590.
19. Zhu, D.; Yan, H.; Liu, X.; Xiang, J.; Zhou, Z.; Tang, J.; Liu, X.; Shen, Y. Intracellularly Disintegratable Polysulfoniums for Efficient Gene Delivery. *Adv. Funct. Mater.* **2017**, *27*, 1606826.
20. Lv, H.; Zhang, S.; Wang, B.; Cui, S.; Yan, J. Toxicity of Cationic Lipids and Cationic Polymers in Gene Delivery. *J. Controlled Release* **2006**, *114*, 100–109.
21. Son, S.; Namgung, R.; Kim, J.; Singha, K.; Kim, W. J. Bioreducible Polymers for Gene Silencing and Delivery. *Acc. Chem. Res.* **2011**, *45*, 1100–1112.
22. Dong, R.; Zhou, Y.; Huang, X.; Zhu, X.; Lu, Y.; Shen, J. Functional Supramolecular Polymers for Biomedical Applications. *Adv. Mater.* **2015**, *27*, 498–526.
23. Hu, J.; Liu, S. Topological Effects of Macrocyclic Polymers: From Precise Synthesis to Biomedical Applications. *Sci. China Chem.* **2017**, *60*, 1153–1161.
24. Xu, C.; Tian, H.; Chen, X. Recent Progress in Cationic Polymeric Gene Carriers for Cancer Therapy. *Sci. China Chem.* **2017**, *60*, 319–328.
25. Cheng, R.; Feng, F.; Meng, F.; Deng, C.; Feijen, J.; Zhong, Z. Glutathione-Responsive Nano-Vehicles as a Promising Platform for Targeted Intracellular Drug and Gene Delivery. *J. Controlled Release* **2011**, *152*, 2–12.
26. Mauriello Jimenez, C.; Aggad, D.; Croissant, J. G.; Tresfield, K.; Laurencin, D.; Berthomieu, D.; Cubedo, N.; Rossel, M.; Alsaiari, S.; Anjum, D. H. Porous Porphyrin-Based Organosilica Nanoparticles for NIR Two-Photon Photodynamic Therapy and Gene Delivery in Zebrafish. *Adv. Funct. Mater.* **2018**, *28*, 1800235.
27. Nguyen, K. T.; Zhao, Y. Engineered Hybrid Nanoparticles for On-Demand Diagnostics and Therapeutics. *Acc. Chem. Res.* **2015**, *48*, 3016–3025.
28. Feng, L.; Zhu, C.; Yuan, H.; Liu, L.; Lv, F.; Wang, S. Conjugated Polymer Nanoparticles: Preparation, Properties, Functionalization and Biological Applications. *Chem. Soc. Rev.* **2013**, *42*, 6620–6633.
29. Slowing, I. I.; Trewyn, B. G.; Giri, S.; Lin, V. Y. Mesoporous Silica Nanoparticles for Drug Delivery and Biosensing Applications. *Adv. Funct. Mater.* **2007**, *17*, 1225–1236.
30. Zhuang, J.; Young, A. P.; Tsung, C. K. Integration of Biomolecules with Metal–Organic Frameworks. *Small* **2017**, *13*, 1700880.
31. Peng, S.; Bie, B.; Sun, Y.; Liu, M.; Cong, H.; Zhou, W.; Xia, Y.; Tang, H.; Deng, H.; Zhou, X. Metal-Organic Frameworks for

DOI: 10.31635/ccschem.019.20180011
CCS Chem. **2019**, *1*, 156–165

Precise Inclusion of Single-Stranded DNA and Transfection in Immune Cells. *Nat. Commun.* **2018**, *9*, 1293.
32. Tian, J.; Zhou, T.-Y.; Zhang, S.-C.; Aloni, S.; Altoe, M. V.; Xie, S.-H.; Wang, H.; Zhang, D.-W.; Zhao, X.; Liu, Y. Three-Dimensional Periodic Supramolecular Organic Framework Ion Sponge in Water and Microcrystals. *Nat. Commun.* **2014**, *5*, 5574.
33. Tian, J.; Xu, Z.-Y.; Zhang, D.-W.; Wang, H.; Xie, S.-H.; Xu, D.-W.; Ren, Y.-H.; Wang, H.; Liu, Y.; Li, Z.-T. Supramolecular Metal-Organic Frameworks That Display High Homogeneous and Heterogeneous Photocatalytic Activity for H_2 Production. *Nat. Commun.* **2016**, *7*, 11580.
34. Tian, J.; Chen, L.; Zhang, D.-W.; Liu, Y.; Li, Z.-T. Supramolecular Organic Frameworks: Engineering Periodicity in Water through Host–Guest Chemistry. *Chem. Commun.* **2016**, *52*, 6351–6362.
35. Tian, J.; Wang, H.; Zhang, D.-W.; Liu, Y.; Li, Z.-T. Supramolecular Organic Frameworks (Sofs): Homogeneous Regular 2d and 3d Pores in Water. *Natl. Sci. Rev.* **2017**, *4*, 426–436.
36. Li, X.-F.; Yu, S.-B.; Yang, B.; Tian, J.; Wang, H.; Zhang, D.-W.; Liu, Y.; Li, Z.-T. A Stable Metal-Covalent-Supramolecular Organic Framework Hybrid: Enrichment of Catalysts for Visible Light-Induced Hydrogen Production. *Sci. China Chem.* **2018**, *61*, 830–835.
37. Chen, Y.; Huang, F.; Li, Z.-T.; Liu, Y. Controllable Macrocyclic Supramolecular Assemblies in Aqueous Solution. *Sci. China Chem.* **2018**, *61*, 979–992.
38. Tian, J.; Yao, C.; Yang, W.-L.; Zhang, L.; Zhang, D.-W.; Wang, H.; Zhang, F.; Liu, Y.; Li, Z.-T. In Situ-Prepared Homogeneous Supramolecular Organic Framework Drug Delivery Systems (Sof-Ddss): Overcoming Cancer Multidrug Resistance and Controlled Release. *Chin. Chem. Lett.* **2017**, *28*, 798–806.
39. Ko, Y. H.; Kim, E.; Hwang, I.; Kim, K. Supramolecular Assemblies Built with Host-Stabilized Charge-Transfer Interactions. *Chem. Commun.* **2007**, *38*, 1305–1315.
40. Zhang, Z.-J.; Zhang, Y.-M.; Liu, Y. Controlled Molecular Self-Assembly Behaviors between Cucurbituril and Bispyridinium Derivatives. *J. Org. Chem.* **2011**, *76*, 4682–4685.
41. Liu, Y.; Yang, H.; Wang, Z.; Zhang, X. Cucurbit [8] Uril-Based Supramolecular Polymers. *Chem. Asian J.* **2013**, *8*, 1626–1632.
42. Biedermann, F.; Nau, W. M.; Schneider, H. J. The Hydrophobic Effect Revisited—Studies with Supramolecular Complexes Imply High-Energy Water as a Noncovalent Driving Force. *Angew. Chem. Int. Ed.* **2014**, *53*, 11158–11171.
43. Lagona, J.; Mukhopadhyay, P.; Chakrabarti, S.; Isaacs, L. The Cucurbit [N] Uril Family. *Angew. Chem. Int. Ed.* **2005**, *44*, 4844–4870.
44. Barrow, S. J.; Kasera, S.; Rowland, M. J.; del Barrio, J.; Scherman, O. A. Cucurbituril-Based Molecular Recognition. *Chem. Rev.* **2015**, *115*, 12320–12406.
45. Yang, H.; Yuan, B.; Zhang, X.; Scherman, O. A. Supramolecular Chemistry at Interfaces: Host–Guest Interactions for Fabricating Multifunctional Biointerfaces. *Acc. Chem. Res.* **2014**, *47*, 2106–2115.
46. Isaacs, L. Stimuli Responsive Systems Constructed Using Cucurbit [N] Uril-Type Molecular Containers. *Acc. Chem. Res.* **2014**, *47*, 2052–2062.
47. Yang, X.; Liu, F.; Zhao, Z.; Liang, F.; Zhang, H.; Liu, S. Cucurbit [10] Uril-Based Chemistry. *Chin. Chem. Lett.* **2018**, *29*, 1560–1566.
48. Zhang, S.; Ye, L.; Zhao, W.; Yang, B.; Wang, Q.; Hou, J. Realizing Over 10% Efficiency in Polymer Solar Cell by Device Optimization. *Sci. China Chem.* **2015**, *58*, 248–256.
49. Yin, Z.-J.; Wu, Z.-Q.; Lin, F.; Qi, Q.-Y.; Xu, X.-N.; Zhao, X. A Supramolecular Bottlebrush Polymer Assembled on the Basis of Cucurbit [8] Uril-Encapsulation-Enhanced Donor–Acceptor Interaction. *Chin. Chem. Lett.* **2017**, *28*, 1167–1171.
50. Li, T.-T.; Wen, L.-L.; Ji, H.-L.; Liu, F.-Y.; Sun, S.-G. Bromination of N-Phenyloxypropyl-N′-Ethyl-4, 4′-Bipyridium in Cucurbit [8] Uril Molecular Reactor. *Chin. Chem. Lett.* **2017**, *28*, 463–466.
51. Yao, C.; Tian, J.; Wang, H.; Zhang, D.-W.; Liu, Y.; Zhang, F.; Li, Z.-T. Loading-Free Supramolecular Organic Framework Drug Delivery Systems (Sof-Ddss) for Doxorubicin: Normal Plasm and Multidrug Resistant Cancer Cell-Adaptive Delivery and Release. *Chin. Chem. Lett.* **2017**, *28*, 893–899.
52. Watson, J. D.; Crick, F. H. Molecular Structure of Nucleic Acids. *Nature* **1953**, *171*, 737–738.
53. Mandelkern, M.; Elias, J. G.; Eden, D.; Crothers, D. M. The Dimensions of DNA in Solution. *J. Mol. Biol.* **1981**, *152*, 153–161.
54. Hardy, J. G.; Kostiainen, M. A.; Smith, D. K.; Gabrielson, N. P.; Pack, D. W. Dendrons with Spermine Surface Groups as Potential Building Blocks for Nonviral Vectors in Gene Therapy. *Bioconjugate Chem.* **2006**, *17*, 172–178.
55. Pattni, B. S.; Chupin, V. V.; Torchilin, V. P. New Developments in Liposomal Drug Delivery. *Chem. Rev.* **2015**, *115*, 10938–10966.
56. Wu, Y.-P.; Yang, B.; Tian, J.; Yu, S.-B.; Wang, H.; Zhang, D.-W.; Liu, Y.; Li, Z.-T. Postmodification of a Supramolecular Organic Framework: Visible-Light-Induced Recyclable Heterogeneous Photocatalysis for the Reduction of Azides to Amines. *Chem. Commun.* **2017**, *53*, 13367–13370.
57. Privalov, P. L. Microcalorimetry of Macromolecules: The Physical Basis of Biological Structures. *J. Solution Chem.* **2015**, *44*, 1141–1161.
58. Silverstein, T. P. The Real Reason Why Oil and Water Don't Mix. *J. Chem. Educ.* **1998**, *75*, 116.

DOI: 10.31635/ccschem.019.20180011
CCS Chem. **2019**, *1*, 156–165